KECK Geology Consortium
Learning Science Through Research
Published by the Keck Geology Consortium
Short Contributions
Keck Geology Consortium
Volume 36
May 2024
doi: 10.18277/AKRSG.2024.36.09

ELUCIDATION OF AN UNDEFINED RELATIONSHIP: A STUDY OF THE BOXELDER CREEK QUARTZITE AND LITTLE ELK GRANITE TO DECIPHER PALEOPROTEROZOIC BASIN DEVELOPMENT IN THE BLACK HILLS, SOUTH DAKOTA

WILLA OBRINGER, Lake Superior State University
Project Advisors: Paul Kelso and Derek Wright

INTRODUCTION

The Black Hills of South Dakota, located on the southeastern edge of the Wyoming Province, are host to an extensive range of complex tectonic events, from the breakup of supercontinent Kenorland to the Trans-Hudson and Laramide orogenies (Whitmeyer & Karlstrom, 2007). In the Late Cretaceous, the Laramide Orogeny uplifted the Black Hills, providing excellent exposure of Archean and Proterozoic terranes (Lisenbee,1988). Two Archean domains are exposed in the Black Hills, the Bear Mountain Domain (BMD) and the Little Elk Granite (LEG) Domain, the latter of which is central to this study. The location of the LEG alone spawns several questions, as it is geographically separated from other Neoarchean rocks of the Wyoming craton (Fig. 1).

Several tectonic models have been proposed to explain the distribution of Neoarchean rocks in the Black Hills. One model suggests that the LEG formed by arc magmatism and represents one of the easternmost exposures of Neoarchean magmatism in the Wyoming Province (Karlstrom & Houston, 1984). In this model, the LEG and BMD formed along the edge of the craton during crustal accretion (Karlstrom & Houston, 1984). The generation of crust in these domains is due to plate convergence between the Superior and Wyoming Cratons and is considered to represent the final assembly of supercontinent Kenorland between 2,590 and 2450 Ma (McCombs et al., 2004). A focal point of this model is the Blue Draw Metagabbro (BDM), variably thought to be evidence of arc magmatism (Van Boening & Nabelek, 2008) or a product of continental breakup and rifting between the Wyoming and Superior cratons at ca. 2.48 Ga (Dahl et al., 2006). The latter theory is associated with conflicting tectonic models, which stand on the premise that subduction was not involved in the tectonic evolution of the Black Hills, but rather rifting events catalyzed by a mantle plume (Van Boening & Nabelek, 2008). One model for the rifting event suggests that two rifting periods exposed Archean domains and formed a basin where Proterozoic sediments were later deposited (Redden et al., 1990). This model suggests that sediment deposition occurred in an extensional setting within the Wyoming craton, with western-sourced sediments filling the basin to the east. This study aims to evaluate the relationship between the LEG and Boxelder Creek Quartzite (BCQ) where they are exposed in Little Elk Creek to assess the plausibility of these various tectonic models.

GEOLOGIC BACKGROUND

The BCQ, characterized as an orthoquartzite with stretched pebble metaconglomerate layers, is suggested to be sourced from Neoarchean crust, including the LEG, during a Paleoproterozoic rifting event (Redden & DeWitt, 2008). The LEG is an augen gneiss with an I-type granite protolith and a Pb-Pb age of 2,559 +/- 6 Ma (McCombs et al., 2004). The exact age of the BCQ has yet to be determined using modern analytical methods and has been bracketed between the LEG and BDM (Redden & DeWitt, 2008). The BCQ is juxtaposed against the LEG by a local shear zone, making the relationship between the two formations unclear. It is unknown whether the granites intrude or are buried by the BCQ.

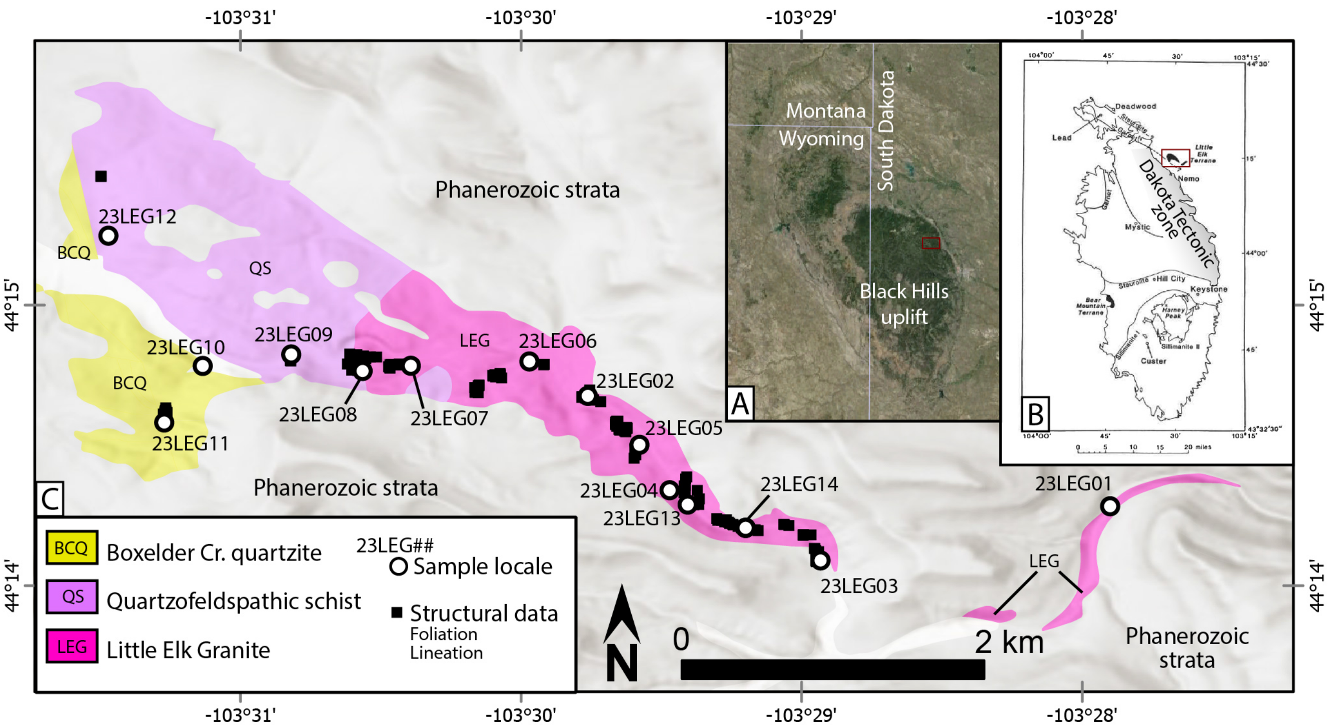

Figure 1. A) Google Earth image showing the location of the Black Hills (dark green region) relative to political borders. The Little Elk Creek area is outline by the red rectangle. B) Metamorphic isograd map of the Black Hills Precambrian core from Gosselin et al. (1988). Black shaded regions represent Archean rocks. The Little Elk Creek area is outline by the red rectangle. C) Geologic map of the Little Elk Creek area showing sample and structural data locations. Modified from Redden and DeWitt (2008).

METHODS

Structural Analysis

Orientations of foliations, clasts, and fold axes were measured using a Brunton Compass. By analyzing the morphology of porphyroclasts, shear sense was recorded. The lengths of maximum and minimum axes of elongated cobbles were collected from the BCQ outcrop in two dimensions, along strike and down-dip within the foliation. Cobble length measurements were entered into the EllipseFit 3.11 program (Vollmer, 2018) to create Hsu and Flinn-Ramsay plots.

Geochemistry

Scanning electron microscopy and micro X-ray fluorescence analysis offered geochemical insights into the BCQ. The back-scattered electron detector (BSD-C) was used to perform compositional analysis through energy dispersive spectroscopy (EDS). The accelerating voltage was set between 20-30 KeV, and a 40-60 probe count was used to observe samples in low vacuum mode. The rhodium X-ray tube with microcapillary optics was used for µXRF analysis, with a dwell time of 25 ms/pixel and a pixel size of 20 micrometers.

Geochronology

Zircon grains retrieved from the BCQ were dated using Laser Ablation-Inductively Coupled Plasma Mass Spectrometry (LA-ICPMS) at the LaserChron Lab at the University of Arizona. Samples were crushed, sieved to less than 250 micrometers, and panned using a miner's gold pan to remove dust and light minerals. Magnetic grains were removed using a hand magnet and Frantz LB-1 isodynamic separator. Lithium heteropolytungstate (LST), with a density of 2.85 g/cc, was used to separate dense non-magnetic minerals (e.g., zircon) from low-density, non-magnetic minerals such as quartz and feldspar.

Zircon grains were mounted with three zircon standards: the Duluth Gabbro (FC1; 1099 ± 2 Ma), Sri Lanka (SL; 563.5 ± 2.3 Ma), and R33 (419.3 ± 0.4 Ma) (Gehrels, 2010). Analysis spots were picked using backscattered electron and cathodoluminescence imaging. A 15 um beam was used, and the laser was set at a repetition rate of 8 Hz and fluence of 4 J/cm2, which ablated at a rate of 1 mm/s and yielded an average pit depth of 12 mm. An uncertainty of

2-sigma (%) is achieved. Data was filtered employing concordance using an 80% threshold. IsoplotR was utilized to generate kernel density estimate plots, calculate the weighted mean age of the youngest statistical population, and plot data on a Wetherill concordia diagram (Ludwig, 2008).

RESULTS

Structural Analysis

Outcrops of the BCQ have a steeply southwest-dipping foliation (126/70º SW) and steeply southwest plunging stretching lineation (Fig. 2A). Several moderately plunging folds are scattered throughout outcrops trending south/southeast (Fig. 2A) and deform the foliation. Conglomerate clasts form sigma porphyroclasts, which indicate top-to-the-left shear-sense parallel to foliation (Fig. 2B). Ramsay plots generated from clast length measurements indicate strain is predominantly in the field of flattening (Fig. 2C), yet the asymmetric porphyroclasts also require a simple shear component to the deformation. Observation of thin sections reveals both static quartz recrystallization textures and undulose extinction, with lesser amounts of bulging grain boundaries. Evidence of ductile shearing is prevalent within thin sections in asymmetric porphyroclasts and S-C fabrics. Asymmetric porphyroclasts and S-C fabrics both indicate top-to-the-left shear sense in thin section.

Geochemistry

SEM and µXRF analyses revealed abundant chromium, nickel, titanium, zinc, iron mineralization and lesser amounts of silver, copper, and rare earth element mineralization (Fig. 3). Chromium and titanium are concentrated in fuchsite and titanite, respectively, and concentrated within micaceous seams surrounding larger, quartz-dominated clasts. Iron and zinc mineralization show no spatial patterns; however, in some instances, iron is mineralized in ooids. Silver traces correlate with sulfur concentrations, suggesting silver is hosted within sulfide minerals such as acanthite. However, there are instances in which silver is associated with iron. Copper is associated with aluminum, silica, and iron within single grains, possibly in the for of aluminum ferrian chrysocolla. Uranium and thorium are

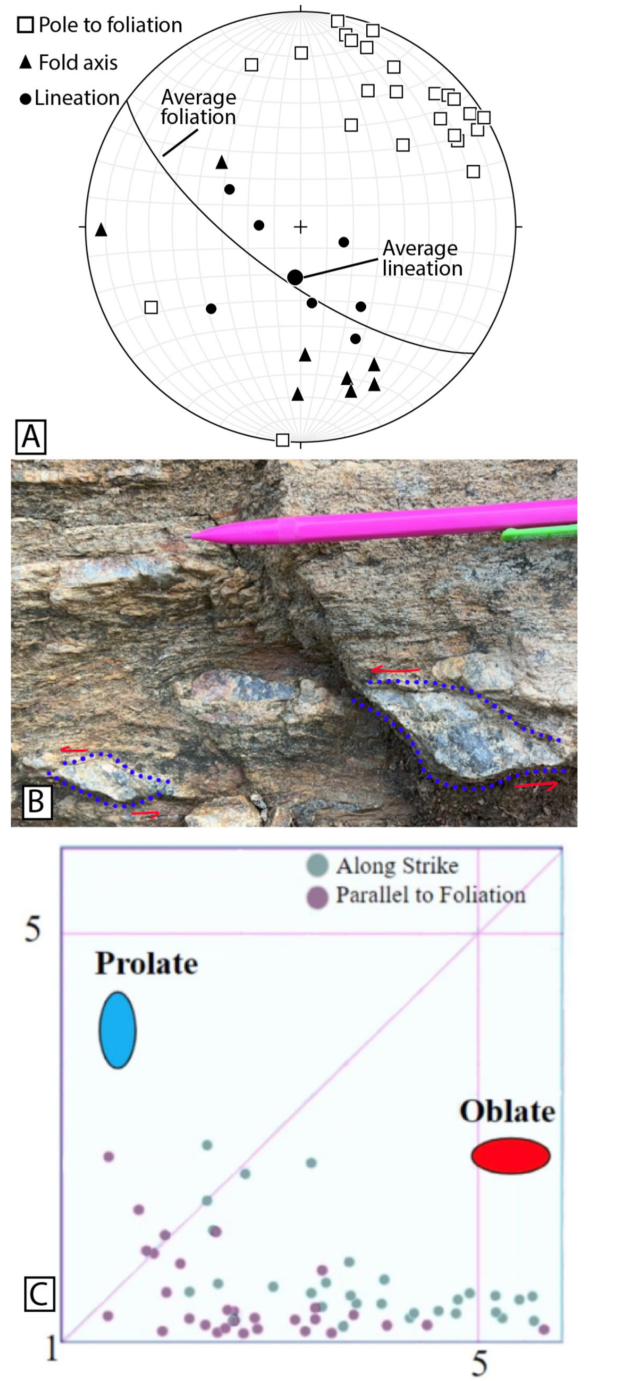

Figure 2. A) Equal area lower hemisphere stereonet showing structural data for the Boxelder Creek Quartzite. B) Outcrop photo showing sheared quartz clasts that indicate left lateral shear sense. C) Ramsay plot showing measurements from the quartz clasts indicating that they plot in the field of flattening.

prevalent within zircon grains.

Rare earth elements are found within monazite and zircon. The light rare earth elements (LREEs) cerium, lanthanum, and neodymium were most common, with only a few cases of ytterbium. LREEs are substituted in exchange for zirconium in zircon and phosphorus in monazite.

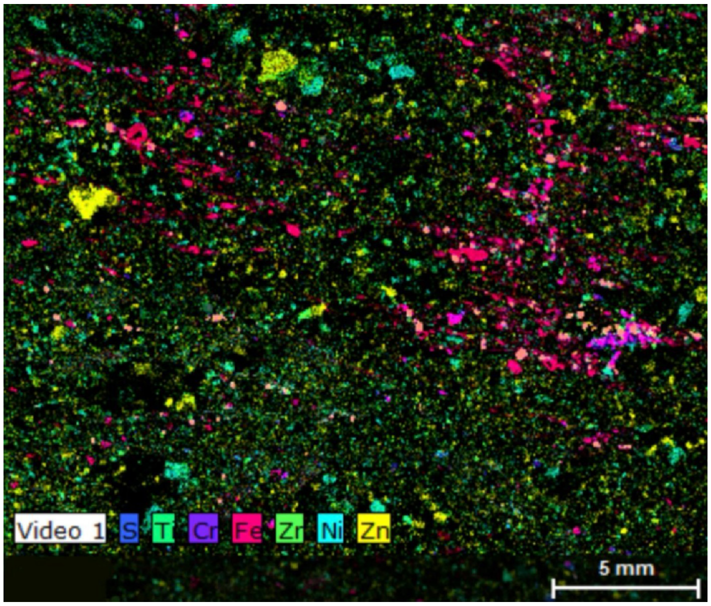

Figure 2. μXRF map displaying trace mineral and metal concentrations within the BCQ. The occurrence of transition metals such as Fe, Ni, and Zn suggests hydrothermal alteration.

Geochronology

Spot analyses (n=182) were generated for the single sample of the BCQ via LA-ICPMS. Sixty-nine of the analyses passed the filtering criteria. The concordia diagram shows both discordant and reverse discordant values (Fig. 4B). Discordant values associated with lead loss yield several ages younger than 2.48 Ga; these values are known to be inaccurate due to the intrusive relationship between the 2.48 Ga BDM and BCQ (Dahl et al., 2006). The KDE of the U-Pb data shows age populations at ca. 2560 Ma, 2700 Ma, 3000 Ma, and 3300 Ma (Fig. 4C). The maximum depositional age of the BCQ is 2552.1 ± 7.1 Ma (Fig. 4D), determined by taking the weighted mean of the youngest age population.

DISCUSSION

Structural Analysis

In field observations, the BCQ displays sheared clasts with top-left kinematics contained within the foliation (Fig. 2B). These clasts record left-lateral simple shear parallel to the foliation plane. This field data, combined with the flattening observed in the Ramsay diagram (Fig. 2C), suggests that these deformation features formed together in left-lateral transpression (e.g., Fossen and Tikoff, 1998). These deformation fabrics most likely record D3 deformation manifested

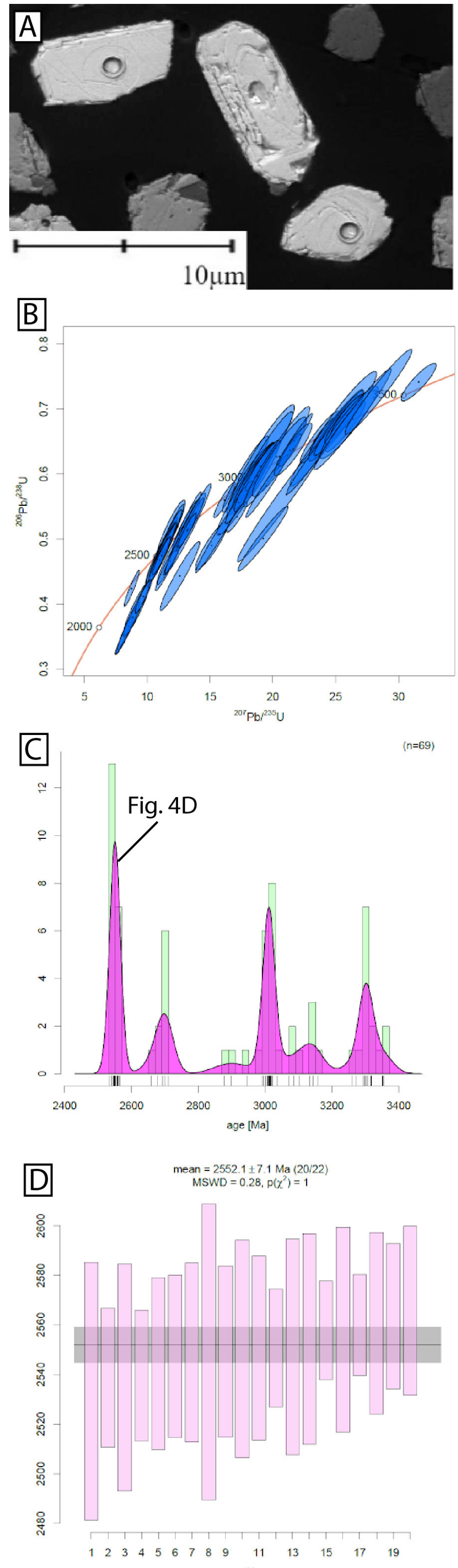

Figure 4. Geochronological data from the Boxelder Creek Quartzite. (A) BSE image of representative zircon grains with laser pits. (B) Wetherill concordia diagram showing the quality of the data that passed the filtering criteria. (C) Kernel density estimate plot showing age populations of detrital zircon grains in the Boxelder Creek Quartzite. (D) Weighted mean plot of the youngest detrital zircon dates in the Boxelder Creek Quartzite.

as a mylonitic sinistral transpression zone, which has also been documented in the LEG across strike of the BCQ (Allard & Portis, 2013).

Geochemistry and Mineralization

Transition metals such as nickel, zinc, copper, silver, and the accessory mineral pyrite are present within the BCQ and were likely mobilized by hydrothermal fluids. Pyrite is present alongside other detrital heavy metals in a mineral assemblage typical within paleoplacer deposits (e.g., Taylor & Anderson, 2010). The quartz pebble conglomerate lithology of the BCQ, along with its deposition within a clastic basin, and late Archean to early Proterozoic age, is observed among several paleoplacer deposits (Taylor & Anderson, 2010).

Sediment Provenance

The BCQ contains zircon age populations at ca. 2560, 2700, 3000, and 3300 Ma (Fig. 4C). The wide range of ages and implied sources for the BCQ is not unexpected, as it is hypothesized to be an alluvial fan and fluvial deposit sourced from the Wyoming craton (Gosselin, 1988; Redden & Dewitt, 2008). The Montana metasedimentary province and the Beartooth-Bighorn magmatic zone are subprovinces within the Wyoming craton with ages up to 3.5 Ga and contain detrital zircons dated up to 4 Ga (Mueller & Frost, 2006), making these a plausible source of the 3000 Ma and 3300 Ma zircon populations in the BCQ. Discordant values on the concordia diagram likely record lead loss from younger metamorphic events.

Discovery of ca. 2.56 Ga detrital zircons within the BCQ confirms that the LEG (2559 ± 6 Ma: McCombs et al., 2004) was a source for sediments within the BCQ. However, the lack of feldspars in thin section and the presence of ultramafic-derived materials spawns further questions. The absence of feldspars can be explained by distinctly different chemical weathering during the Archean. During this period, increased rainfall, higher temperatures, and higher atmospheric CO_2 (Hessler & Lowe, 2006) may have enhanced feldspar weathering relative to modern rates, leaving a quartz-dominated source for the BCQ. The abundance of heavier elements, including Cr (Fig. 3), suggests that the source terrain for the BCQ was not only granitic but likely included mafic-ultramafic sources as well. The presence of iron oxide clasts suggests that the Nemo Iron formation was a source alongside the LEG and other granitic material within the Wyoming craton.

Synthesis

This study establishes that the BCQ records basin formation between 2560 and 2480 Ma, aligning with the hypothesized breakup of the supercontinent Kenorland (McCombs et al., 2004). SEM and µXRF analyses reveal abundant chromium, nickel, titanium, zinc, iron, and smaller amounts of silver, copper, and rare earth elements. Exhumation and sedimentary recycling of mantle materials during this rifting event are possible sources of these elements. The prevalence of these transition metals could also suggest hydrothermal alteration linked to a rift environment (Redden, 1987; Taylor & Anderson, 2010). The Archean cratonic setting, age, lithology, and distinct mineralization of the BCQ support the hypothesis that the BCQ is a paleoplacer deposit (e.g., Redden, 1987). Ramsay diagrams show flattening as the primary strain, and sinistral kinematic indicators are abundant in outcrops and thin sections, indicating the BCQ deformed by sinistral transpressional shear. Fabrics in the BCQ are likely related to D3 in the Black Hills, which is shared with the LEG across strike of the shear zone (Allard & Portis, 2013). Conclusively, the data presented here support the interpretation that the BCQ formed in a rift environment that received detritus from the LEG and other parts of the Wyoming craton between 2560-2480 Ma. Following closure of the ocean basin in the Paleoproterozoic, left lateral transpression recorded in the BCQ is shared with the LEG, suggesting that the shear zone between them is a relatively minor structure that overprints a depositional relationship between the BCQ and LEG.

ACKNOWLEDGMENTS

This material is based upon work supported by the Keck Geology Consortium and the National Science Foundation under Grant No. 2050697. NSF 2215270 MRI: Acquisition of a low vacuum Scanning Electron Microscope (SEM) with EDS detector and STEM capability to advance research and undergraduate research training. NSF 2320397 Equipment: MRI: Track 1 Acquisition of a Micro X-ray Fluorescence Spectrometer to Support Multidisciplinary Research and Education in the Upper Midwest. NSF-EAR 2050246 for support of the Arizona LaserChron Center. I want to thank my mentor, Dr. Trevor Waldien, for imparting extensive knowledge on all aspects of geology and preparing me for the professional world. Additionally, I express my appreciation to Dr. Paul Kelso and Dr. Derek Wright, professors at Lake Superior State, for their guidance, knowledge, and assistance.

REFERENCES

Allard, S. T., & Portis, D. H. (2013). Paleoproterozoic transpressional shear zone, eastern Black Hills, South Dakota: Implications for the late tectonic history of the southern Trans-HudsonOrogen. Rocky Mountain Geology, 48(2), 73-99.

Corrigan, David & Pehrsson, S. & Wodicka, N. & Dekemp, E. (2009). The Palaeoproterozoic Trans-Hudson Orogen: A prototype of modern accretionary processes. Geological Society, London, Special Publications. 327. 457–479. 10.1144/SP327.19.

Dahl, P. S., Hamilton, M. A., Wooden, J. L., Foland, K. A., Frei, R., McCombs, J. A., & Holm, D. K.(2006). 2480 Ma mafic magmatism in the northern Black Hills, South Dakota: a new link connecting the Wyoming and Superior cratons. Canadian Journal of Earth Sciences, 43(10),1579–1600.

Fossen, H. and Tikoff, B. (1998). Extended Models of Transpression and Transtension, and Application to Tectonic Settings. In: Holdsworth, R.E., Strachan, R.A. and Dewey, J.F., Eds., Continental Transpressional and Transtensional Tectonics. Geological Society of London, Special Publications, 135, 1–14.

Gehrels, G. (2010). U-Th-Pb analytical methods for Zircon. Arizona LaserChron Center. https://sites.google.com/laserchron.org/arizonalaserchroncenter/home.

Gosselin, D. C., Papike, J. J., Zartman, R. E., Peterman, Z. E., & Laul, J. C. (1988). Archean rocks of the Black Hills, South Dakota: Reworked basement from the southern extension of the Trans-Hudson orogen. Geological Society of America Bulletin, 100(8), 1244-1259.

Hessler, A. M., & Lowe, D. R. (2006). Weathering and sediment generation in the Archean: An integrated study of the evolution of siliciclastic sedimentary rocks of the 3.2Ga Moodies Group, Barberton Greenstone Belt, South Africa. Precambrian Research, 151(3–4), 185–210. https://doi.org/10.1016/j.precamres.2006.08.008

Karlstrom, K. E., & Houston, R. S. (1984). The Cheyenne Belt: Analysis of a Proterozoic suture in southern Wyoming. Precambrian Research, 25(4), 415-446.

Lisenbee, A. L. (1988). Tectonic history of the Black Hills uplift. AAPG Field trip guide to the Powder River Basin.

Ludwig, K. R. (2008). User's manual for Isoplot 3.70 (Vol. 4, pp. 76–80). Berkeley Geochronology Center Special Publication. https://doi.org/10.1111/j.1439-0272.2007.00823.x

McCombs, J.A., Dahl, P.S., & Hamilton, M.A. (2004). U–Pb ages of Neoarchean granitoids from the Black Hills, South Dakota, USA: implications for crustal evolution in the Archean Wyoming province. Precambrian Research, pp. 130, 161–184.

Nicosia, C. & Allard, S., (2014). Petrologic and Geochemical Characterization of Archean Gneisses in the Little Elk Terrane, Black Hills, South Dakota. Student Research and Creative Projects 2014-2015. 11.

Mueller, P.A. and C D Frost. 2006. The Wyoming Province: a distinctive Archean craton in Laurentian North America. Canadian Journal of Earth Sciences. 43(10): 1391-1397. https://doi.org/10.1139/e06-075

Redden, J.A. (1987)."Uraniferous Early Proterozoic Conglomerates of the Black Hills, South Dakota, USA." Geological Survey, Denver, Colorado, United States of America.

Redden, J. A., Peterman, Z. E., Zartman, R. E., DeWitt, E., (1990). U-Th-Pb geochronology and preliminary interpretation of Precambrian tectonic events in the Black Hills, South Dakota, in Lewry, J. F., and Stauffer, M. R., eds., The Early Proterozoic Trans-Hudson Orogen of North America: Geological Association of Canada Special Paper 37, p. 229–251.

Redden, J.A., and DeWitt, E. (2008). Maps Showing Geology, Structure, and Geophysics of the Central Black Hills, South Dakota: U.S. Geological Survey Scientific Investigations Map 2777, 44-p. pamphlet, 2 sheets, https://pubs.usgs.gov/sim/2777/ (accessed September 2023).

Taylor, R.D., and Anderson, E.D., (2010). Quartz-Pebble-Conglomerate Gold Deposits, Chapter P of Mineral Deposit Models for Resource Assessment, U.S. Geological Survey Scientific Investigations Report 2010–5070–P.

Van Boening, A. M., & Nabelek, P. I. (2008). Petrogenesis and tectonic implications of Paleoproterozoic mafic rocks in the Black Hills, South Dakota. Precambrian Research, 167(3-4), 363-376.

Vollmer, F.W., (2018). Automatic contouring of geologic fabric and finite strain data on the unit hyperboloid. Computers & Geosciences. http://dx.doi.org/10.1016/j.cageo.2018.03.006 .

Whitmeyer, S. J., & Karlstrom, K. E. (2007). Tectonic model for the Proterozoic growth of North America. Geosphere, 3(4), 220-259.